5.2 SPACEBORNE SCANNER IMAGING SYSTEM ERRORS

Arun Prakash (General Electric)

INTRODUCTION

There are various stages and forms of error in a spaceborne scanner imaging system. The instrument, in this case consisting of the spacecraft and its sensors, is designed to behave in a nominal or ideal way. In real operating conditions, there are deviations from this nominal behavior. These deviations are a source of error not only as independent entities but because of the interdependence of the various components of the instrument. Thus, deviation from design of one parameter may cause another to display nonoptimal behavior.

The deviations mentioned above are large enough that if they are ignored in subsequent processing on the ground, the resulting images will be distorted and misregistered to unacceptably high levels. Therefore, direct or indirect measurement of deviations in instrument performance is necessary. Inaccuracies in measurements form a source of error which ultimately filter through to the output image along with ground processing errors.

In this paper we will discuss errors due to deviation from ideal instrument performance and due to the measurement system. The discussion will be within the Landsat-D system framework which consists of the spacecraft and two scanner type sensors—the Thematic Mapper (TM) and the Multispectral Scanner (MSS) [1,2].

Whatever the source of error in the instrument, when it propagates through to the image the error can be classified as either radiometric error or geometric error. On ground, it is difficult to distinguish between these two forms of error but from the point of view of the instrument, there is no difficulty in making this classification. In this paper we discuss only those instrument components which contribute to geometric error, because radiometric error is a function of parameters that are largely independent of the instrument being a scanner type or not.

Geometric error implies lack of accurate knowledge of the position of a sample. To place a detector sample of the spacecraft sensor precisely on ground, one needs to know the time the sample was taken, the position of the spacecraft, its orientation (in inertial space) and the orientation of the sensor body with respect to the spacecraft all at that same time. These are the platform or spacecraft components of the imaging system that need to be known. In addition, the sensor characteristics and dynamics need to be known for all time. Other important components which will not be specifically discussed here are earth shape, spin, atmospheric effects, etc.

The next section discusses the platform errors and Section III covers the sensor errors. For convenience, Table 1 shows the units often used interchangeably in describing the errors.

II. PLATFORM ERRORS [7,8,9,11]

With the exception of spacecraft jitter, all platform errors vary slowly (low-frequency error) with respect to the time required to collect data for

one image. The direct effect of these errors on the image is a shift or registration error as opposed to distortion of features within an image. We now discuss the four components of platform error individually, remembering that the Landsat-D System framework is assumed.

Time [7]

The spacecraft clock is updated once every 24 hours from the ground. The accuracy of the updated time is ±3 milliseconds. In a 24-hour period, the clock can also drift by a maximum of ±17 msecs. Thus a maximum of ±20 msec inaccuracy can build up in the spacecraft clock This time error is essentially a bias for any one image and may be treated as a spacecraft or image position knowledge uncertainty.

Ephemeris [7,8,9]

The nominal spacecraft orbit parameters and deviations from them are shown at the bottom of Table 2. At the top of the table is shown the error incurred in measuring the spacecraft ephemeris. This is the measurement error incurred when ephemeris information is uplinked from the ground. In the GPS modes, these errors would reduce substantially. The along-track and cross-track position error directly results in an image registration error, whereas the altitude deviation causes the ground projected pixel size to vary.

Attitude [7,8,9,10,11]

The nominal attitude of the spacecraft implies geocentric pointing of the sensor optical axis. For the Landsat-D TM, the attitude errors are shown in Table 3, along with jitter errors (which are high-frequency attitude errors). The spacecraft attitude control is in error by 36 arc sec [1]. This is a low-frequency error, as shown. The TDRSS antenna drive interacts with the spacecraft structure and causes attitude/jitter error of the magnitude shown. It should be noted that most of this error is in the lower-frequency range and can be measured by the gyros.

High-frequency jitter in the spacecraft is caused by the scanners themselves. Odd harmonics of the scan mirror frequency (7 Hz for the TM and 13.62 Hz for the MSS) are fed back to the sensors through the spacecraft structure. An angular displacement sensor (ADS) is used to measure this jitter on the TM sensor. In Table 3, the baseline and the worst case design values for jitter in the roll, pitch, and yaw axis is given. Error in ADS and DRIRU (dry rotor inertial reference unit) calibration causes measurement error in attitude/jitter.

Alignment [7,8]

The spacecraft assumes a predetermined alignment between the pointed axis and the master reference cube in order to achieve proper pointing. This predetermined alignment can, however, be achieved to within only a certain tolerance, and the real alignment can be measured to only a certain accuracy. The values are shown in Table 4. Another error source in alignment is the fact that it does not remain constant. There is a dynamic component to it caused mainly by thermal bonding due to spacecraft temperature changes. The static error component of alignment results in the sensor pointing away from nominal and is

equivalent to an attitude error. The dynamic component has a time constant that is large enough (about 360 secs) that the resulting error over one image is essentially constant. Both result in image registration errors.

Table 5 shows the approximate geometric errors (in meters) in knowledge of the position of an image due to platform errors. These errors are essentially constant for one image and therefore result in image misregistration. The attitude error shown here is the result of the low-frequency (<2-Hz) attitude errors. Higher-frequency attitude errors (jitter) affect the scan profile and will be dealt with in the next section. Note that the alignment error can be extremely large but postlaunch calibration will reduce this error substantially.

III. SENSOR ERRORS [5,6,8,9]

In this section errors in the sensor are discussed. Some of these errors are a result of platform errors such as spacecraft altitude or jitter. Others are errors in the sensor itself. Specific errors will be discussed with respect to the TM and the MSS will be indicated. As background, the article by Blanchard and Weinstein [3] on the TM design provides a good review of the essential design components of a scanner imaging system.

One advantage of a scanning sensor over nonscanning kinds is that object plane scanning can be used. This simplifies the performance requirements for the rest of the optical system by requiring the telescope to operate at only very small field angles. Moreover, the same zone of each element is used at all scan angles which eliminates many of the major problems of off-axis imaging. The scanning mechanism, however, is also a major source of error in these sensors. Ideally, the samples from all the scans should form an evenly sampled grid on the ground. Deviations from this idealization must be measured in real time so that appropriate ground processing can be applied. In order to understand these deviations, schematics of the MSS and TM sensor mechanisms are shown in Figures 1 and 2.

The MSS design is relatively straightforward. Fiber optics are used to transmit the focused image energy to the detectors. There are four bands with six detectors per band. Sampling of the detector outputs is done only during a scan mirror forward scan. The reverse scan is used to bring the mirror back to its initial position only.

The TM, on the other hand, does its imaging during both forward and reverse scans. Due to the relative velocity between the Earth and the spacecraft in the in-track direction, the forward and reverse scans when projected to earth are skewed to each other. Another scan mirror (the Scan Line Corrector) that opposes the relative in-track motion, is used to compensate for this effect. The TM has seven bands and a total of 100 detectors. These detectors are directly placed on the focal plane; thus fiber optic relays with their attendant losses are bypassed. Spacing between bands is naturally larger in such a design -- up to 183 samples maximum (compared to a maximum of six samples for the MSS). Scan profile repeatability and precise timing is therefore critical for accurate band-to-band registration.

The mirror mechanism that does the scanning is a major source of error in these sensors -- for the TM, this means the scan mirror and the scan line

corrector mirror. During active scan (when imaging is done) the scan mirror design dictates that no torques act on it. Under these conditions, the scan mirror moves at a constant angular velocity in inertial space. This velocity is predetermined by design. The scan line corrector mirror is also designed to scan with a constant angular velocity opposing the in-track velocity of the spacecraft with respect to the Earth. The design of the scan line corrector angular velocity is based on the spacecraft altitude and velocity.

Deviations from design conditions of the scan mechanism result in in-track and cross-track efforts. We will discuss these errors in terms of the scan profiles.

Cross-Track Profile

These are the profile errors in the scan mirror motion. Again, the TM is used as a base to describe the errors. Two kinds of errors occur. Design conditions of torque-free inertial motion result in evenly spaced samples on ground (ignoring the earth curvature effects and slant range effects) and a linear mirror angle versus time plot (profile). Due to small residual torques, however, a nonlinear profile is actually achieved. This means that the mirror motion is faster or slower than nominal and results in ground sample spacings that are uneven. Cross-track profile nonlinearity of the scan line corrector also adds to the total cross-track profile linearity. However, the scan line corrector nonlinearity is largely in the in-track direction.

The other error is called line length error, and refers to deviations that occur in total active scan time with respect to the nominal of 60743 usec. The sources of this error are the control system, spacecraft jitter in the roll axis, and interaction of the two. The sensor scan mirror control system responds very well to jitter caused by itself but poorly to external jitter sources.

The cross-track profile nonlinearity and the line length are dynamic error sources and must be measured in flight. Line length is easily measured by clock counts taken from start to end of scan. The scan mirror cross-track profile for the TM is modeled as a six-term power series with time as the independent variable. It has been shown by extensive tests [6] that the variation in the profile can be accurately modeled by updating the first-order and second-order terms of the power series. This requires knowledge of first-half and second-half scan times which are measured by a clock on the spacecraft. Time is normalized using line length and jitter data.

Table 6 shows the magnitude of along scan (or cross-track) errors.

Along-Track Profile

The ground projected scan profile (i.e., the envelope of the projection of all detectors of a band on ground during one complete scan) should ideally be rectangular, with each scan starting where the last left off. The real ground projected scan profile doesn't follow this simple geometry. Gaps between scans (underlaps) and scan overlaps are present for a number of reasons.

The projected size of a pixel is directly related to the distance between the detector and look point on the Earth's surface. At the spacecraft design altitude of 705.3 km, a detector (42.5 μradians) projects to ground as a 30-meter square pixel. The slant range being larger than the nadir, the scan profile is wider at the ends than it is in the center. This effect is called the bow-tie effect and results in a small scan overlap at the scan ends and an underlap at scan center.

Spacecraft altitude variations (696 km to 741 km) affect the scan profile in two ways. First, as described above, it causes a scan overlap/underlap. The second error is due to spacecraft velocity variations as a result of altitude deviations. The scan line corrector mirror rate design is based on the spacecraft velocity. When the latter changes, the scan line corrector compensation is no longer correct. The forward and reverse scans then are skewed to each other.

Spacecraft jitter in the yaw and pitch axis also shows up in the ground projected scan profile. High-frequency jitter causes underlap/overlap to vary across the scan. See Table 7 for numerical values for scan gap error.

The profiles of the scan mirror and scan line corrector mirrors in the in-track direction is a fixed function known a priori, and, though it does make the ground projected scan profile deviate from the rectangular case, it is a constant, known deviation.

Knowledge of imaging geometry along with measurement of the parameters mentioned above (which cause in-track scan nonlinearities) allows one to accurately describe the scan shape and position of samples on the ground. The next step is to define an algorithm to perform image resampling under the conditions, which will not be discussed in this paper.

Other sources of error in the sensor are detector alignment and the electronics. These errors are relatively small in comparison to the scan nonlinearities. They are summarized in Table 8 and will be briefly discussed. The effective focal length (EFL) of the optical system determines the dimensions of the projection of the detector on ground. Because the image is scanned across the detector arrays, the EFL is also responsible for the system transfer function. Tolerances must be tight if the real sampling is to mimic the design transfer function characteristics. Values for the EFL fabrication and measurement tolerances are shown, as is deviation of EFL.

The spacing between detector arrays for the different bands determines the band-to-band image spacing. Alignment between detector arrays must be within strict tolerance limits or band-to-band registration will suffer.

Vibration of the detector layout causes band-to-band error for band-to-band vibration and also overlap/underlap error for vibration within any one band. The electronics of the system introduces errors too. Detector response nonuniformity is one reason. The filter response and timing errors are other causes. The vibration and detector/electronics responses cause distortions within an image.

This overview of spaceborne scanner imaging system errors shows the sensitivity of image errors to spacecraft component errors and also the interdependance

of the imaging system components. As more sophisticated imaging systems are developed, with greater resolution capabilities and stricter accuracy requirements, the need to understand and model these error sources becomes more important [4].

Table 1. **UNITS**

TM PIXEL = 42.5 μ RAD = 8.77 ARC-SEC ⇒ 30 METERS AT 705.3 KM

MSS PIXEL = 117.2 μ RAD = 24.17 ARC-SEC ⇒ 82.7 METERS AT 705.3 KM

1 μ RAD ⇒ .71 METER AT 705.3

1 ARC-SEC ⇒ 3.4 METER AT 705.3

1 ARC-SEC = 4.85 μ RAD

Table 2. **EPHEMERIS ACCURACY AND VARIATION**

- ORBIT SUPPORT COMPUTING DIVISION EPHEMERIS ERROR

	(1σ AFTER 2 DAYS)	
	POSITION (METERS)	VELOCITY (METERS/SEC)
ALONG TRACK	500*	.163
CROSS TRACK	100	.065
RADIAL	33	.650*

*GSFC SPEC

- VARIATION FROM NOMINAL
  - ALTITUDE (705.3 KM ORBIT): 696 TO 741 KM OVER EARTH; RANGE OF 19 KM OVER ANY FIXED LATITUDE
  - CROSS TRACK: ± 4 KM AT THE EQUATOR
  - INCLINATION: 98.21 ± .045 DEGREES

- SPACECRAFT CLOCK ACCURACY ± 20 MILLISECONDS

Table 3.

ATTITUDE/JITTER ERROR (AT THE TM)

FREQUENCY RANGE	ERROR MAGNITUDE (ARC-SEC)		COMMENT
0 - 0.01 Hz	36 (1σ)		ALL AXES, ATTITUDE CONTROL ERROR
0.01 - 0.4 Hz	10 (1σ)		ALL AXES, TDRSS ANTENNA DRIVE ERROR
0.4 - 7 Hz	0.3 (1σ)		ALL AXES, TDRSS ANTENNA DRIVE ERROR
	BASELINE MODEL (.01 DAMPING)	WORST CASE DESIGN	
>7 Hz	R 0.93 (1σ)	20.0 (PEAK)	ADS LIMIT IS 50 ARC-SEC
	P 0.20 (1σ)	. (PEAK)	LIMITS JITTER GAP TO LESS THAN ONE PIXEL
	Y 0.30 (1σ)	16.8 (PEAK)	LIMITS JITTER GAP TO LESS THAN ONE PIXEL
ADS CALIBRATION REQUIREMENT		3% ERROR	.5 ARC-SEC (1σ) USED IN ERROR BUDGETS
DRIRU CALIBRATION REQUIREMENT		3% ERROR	.5 ARC-SEC (1σ) USED IN ERROR BUDGETS
ATTITUDE DATA PROCESSING REQUIREMENT		1% ERROR	.5 ARC-SEC (1σ) USED IN ERROR BUDGETS

ADS: ANGULAR DISPLACEMENT SENSOR
DRIRU: DRY ROTOR INERTIAL REFERENCE UNIT
TDRSS: TRACKING AND DATA RELAY SATELLITE SYSTEM

Table 4. **STATIC ALIGNMENT**

- **ALIGNMENT REQUIREMENTS**
  - **ALIGNMENT BETWEEN ACS AXIS AND POINTED AXIS WITHIN 1.25 DEGREES (3σ)**
  - **POINT THE AVERAGED AXES OF THE MSS AND TM**
  - **ALIGNMENT KNOWLEDGE ACS TO TM OPTICAL AXIS ROLL = .10, PITCH = .21, YAW = .21 DEGREES (3σ)**
- **POST LAUNCH ESTIMATION OF SPACECRAFT STATIC ALIGNMENT WILL BE PERFORMED**

ACS: ATTITUDE CONTROL SYSTEM

DYNAMIC ALIGNMENT

- **SPACECRAFT TEMPERATURE CHANGES CAUSE ALIGNMENT CHANGES**
  - **EXAMPLE: 1 DEGREE GRADIENT ACROSS THE INSTRUMENT MODUL CAUSES A 12 ARC-SEC ACS TO TM ALIGNMENT CHANGE. (GODDARD ANALYSIS)**

Table 5.

GEOMETRIC ERROR IN SYSTEMATIC CORRECTION DATA (APPROXIMATE)

ERROR SOURCE	CROSS TRACK (METERS 1σ)	ALONG TRACK (METERS 1σ)
EPHEMERIS	100	500
TIME		80
ATTITUDE	123	123
ALIGNMENT	427*	855*
TOTAL (ROOT-SUM-SQUARE)	455 (25 PIXELS 90%)	1001 (55 PIXELS 90%)

*SUBSTANTIAL REDUCTION WILL OCCUR AFTER POSTLAUNCH CALIBRATION

Table 6.

SCAN MIRROR PROFILE

- SCAN MIRROR ALONG SCAN NONLINEARITY DEFINED BY 5TH-ORDER POLYNOMIAL
  - NOMINAL NONLINEARITY 35 MICRORADIAN
- ALONG SCAN PROFILE VARIATIONS
  - ± 10 MICRORADIAN WANDER OVER 2000 SCANS
  - ± 50 MICRORADIAN SHIFT DUE TO A VIBRATION EVENT
  - ± 200 MICRORADIANS WORST CASE SHIFT
- ALONG SCAN CORRECTION
  - LINEAR CORRECTION MEASURED BY SCAN TIME
  - SECOND-ORDER CORRECTION MEASURED BY MIDSCAN TIME
  - JITTER MOVES INERTIAL START, MID, END SCAN POSITIONS
- CROSS SCAN PROFILE MUST BE CORRECTED

NOTE: ALL ANGLES ARE IN OBJECT SPACE

Table 7. **SCAN GAP** ERROR**

ALTITUDE VARIATION	JITTER	TM UNDERLAP/OVERLAP
696 – 741 KM FOR 705.3 ORBIT 713 KM TM DESIGN ALTITUDE	LESS THAN 1 PIXEL	0.2 PIXEL (SPEC)

END SCAN GAP

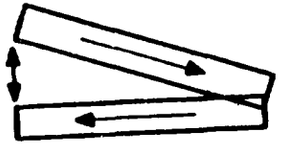

EARTH LOCATION	WORST CASE END SCAN GAP IN PIXELS*
NORTHERN HEMISPHERE	-0.7 TO 0.8
45°N	-0.4 TO 0.6
EQUATOR	-0.2 TO 0.8
45°S	-0.9 TO 0.1
SOUTHERN HEMISPHERE	-1.6 TO 0.8

WORST CASE GAP RANGE

-2.8 TO 2.0

*INCLUDES SCAN WIDTH, SCAN LINE CORRECTOR AND BOWTIE EFFECTS

**GAP < 0 : OVERLAP
= 0 : NOMINAL
> 0 : UNDERLAP

Table 8. Summary of Error Sources

Error Source	Magnitude		
		µrad (90%)	
Effective Focal Length (EFL)	Band	Across-Track	Along-Track
EFL Measurement and Fabrication	1 to 4	2	2
	5 to 6	2	2
	5 to 1	2	2
EFL Deviation	2 µrad (max)		
Focal Plane Tolerance	0.4 µrad (max)		
Detectors			
		µrad (90%)	
Detector Array Alignment Accuracy	Band	Across-Track	Along-Track
	1 to 4	3	3
	5 to 6	31	31
	5 to 1	6	6
Band-to-Band Vibration	1 to 4	1.5	1.5
	5 to 6	1.5	1.5
	5 to 1	1.5	1.5
One-Band Vibration	2.6 µrad random error (90%) in tests.		
Detector Response Nonuniformity	1 to 5	2	2
	5 to 6	8	8
	5 to 1	2	2
Filter Response - Forward to Reverse Scan	Bands 1-5 and 7	1.3 IFOV offset	
	Band 6	5.2 IFOV offset	
Filter Response - Bands 1-5 and 7 to Band 6	3.0 IFOV offset		

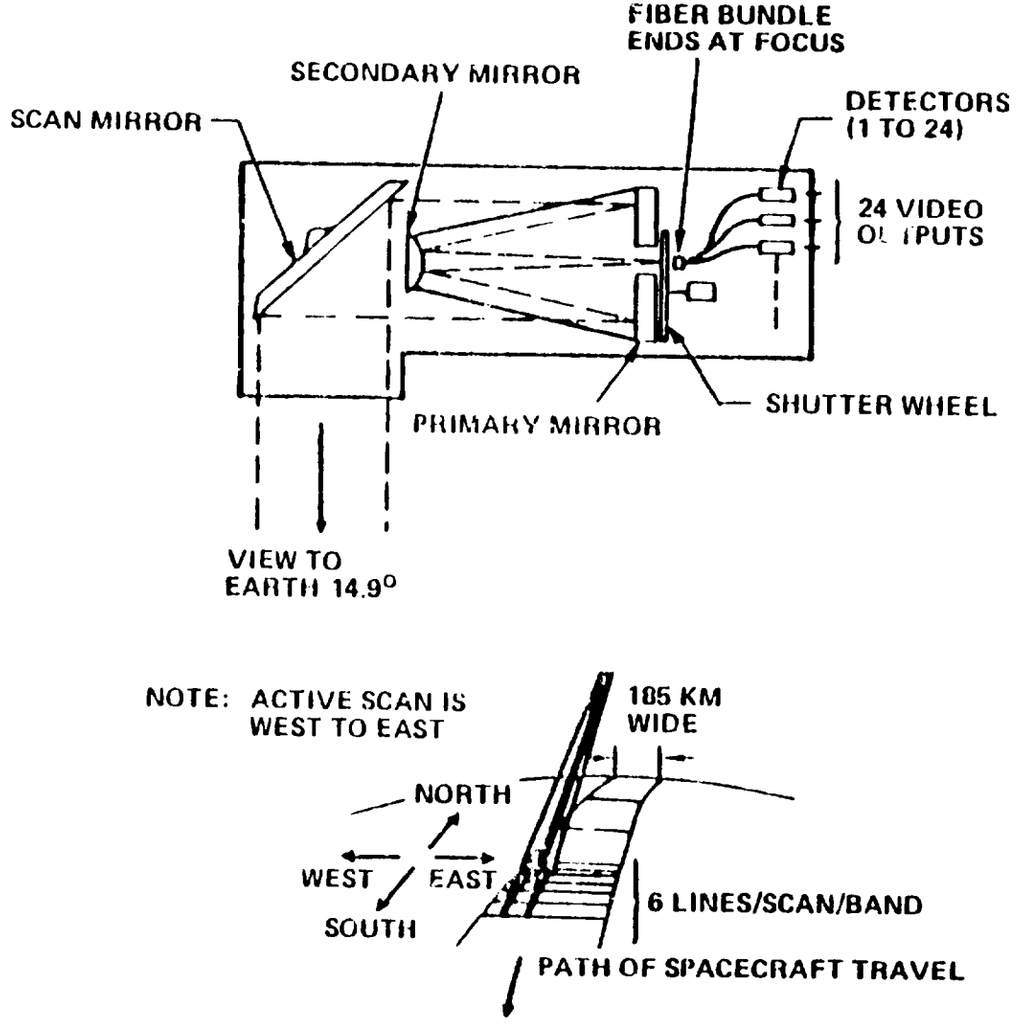

Figure 1. Multispectral Scanner

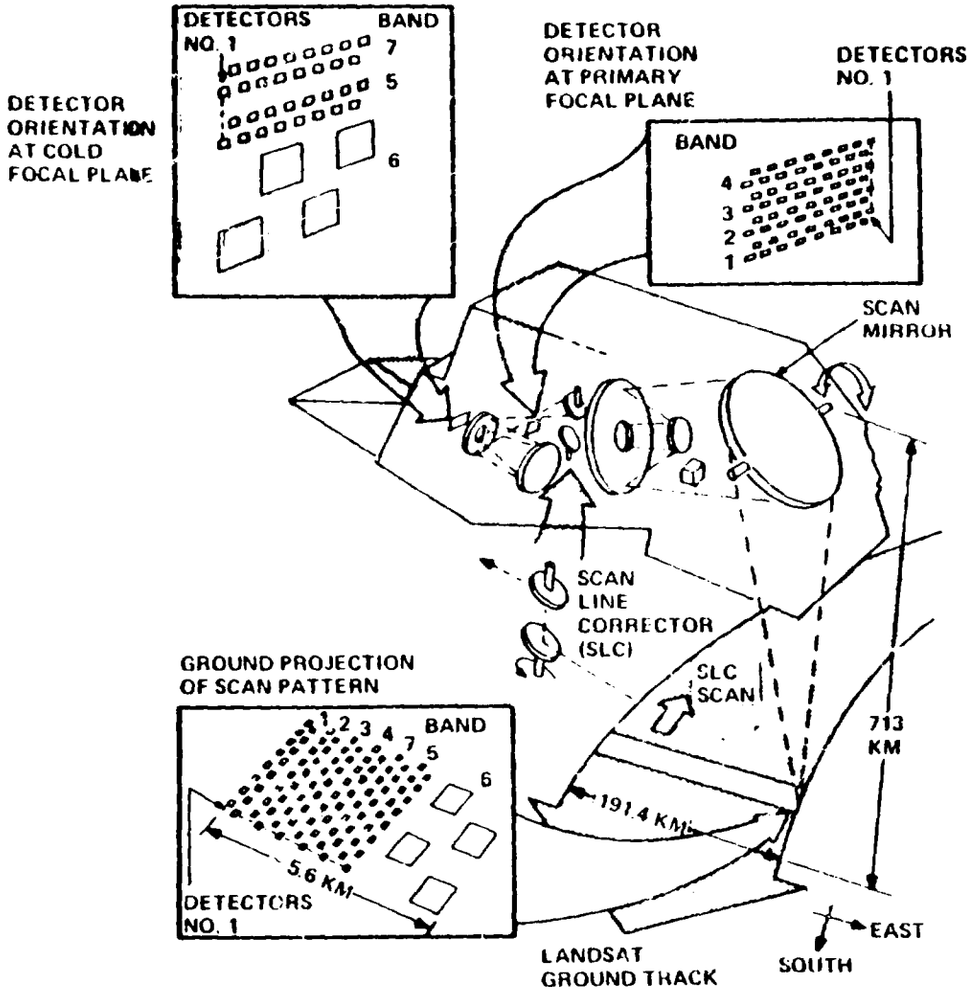

KEY GEOMETRIC FEATURES

- SCAN MIRROR
  - BI DIRECTIONAL CROSS-TRACK SCANNING
  - DATA AVAILABLE TO GROUND:
    - SCAN START TIME
    - SCAN DIRECTION
    - FIRST HALF-SCAN TIME ERROR
    - SECOND HALF-SCAN TIME ERROR
- SCAN LINE CORRECTOR
  - PROVIDES IN TRACK SCANNING
- TWO FOCAL PLANE ASSEMBLIES
- INSTANTANEOUS FIELD OF VIEW (IFOV)
  - BANDS 1-5, 7: 42.5 μrad (30 METERS)
  - BAND 6: 170 μrad (120 METERS)

Figure 2 . Thematic Mapper

REFERENCES

1. V.V. Solmonson, P.L. Smith, Jr., A.B. Park, W.C. Webb, and T.J. Lynch, "An Overview of Progress in the Design and Implementation of Landsat-D Systems", IEEE Trans. on Geoscience and Remote Sensing, Vol. GE-18, No. 2, pp. 137-146, April 1980.

2. T.C. Aepli and W. Wolfe, "Landsat-D the Next Generation System", Western Electronic Show and Convention, Sept. 18-20, 1979.

3. L.E. Blanchard and Oscar Weinstein, "Design Callenges of the Thematic Mapper", IEEE Trans. on Geoscience and Remote Sensing, Vol. GE-18, No. 2, pp. 146-160, April 1980.

4. Roger A. Holmes, "Processing System Techniques for the 80's", Proceedings of the 7th Intl. Symp. on Machine Processing of Remotely Sensed Data, Session II.C. Preprocessing and Systems, pp. 140-145, June 23-26, 1981.

5. A. Prakash and E.P. Beyer, "Landsat-D Thematic Mapper Image Resampling for Scan Geometry Correction", Proceedings of the 7th Intl. Symp. on Machine Processing and Remotely Sensed Data, Session II.C. Preprocessing and Systems, pp. 189-200, June 23-26, 1981.

6. Hughes Aircraft Company, Thematic Mapper Detailed Design Review Package, Hughes No. D4596-SCG 80201R, June 1978.

7. A. Prakash, Landsat-D System Geometric Error Budget, General Electric Co., PIR 1K50-LSD-784B, March 20, 1981.

8. General Electric Company, Landsat-D Thematic Mapper Image Processing System Design Review, Oct. 6-7, 1981.

9. General Electric Company, Landsat-D Multispectral Scanner Image Processing System Design Review, Oct. 6-7, 1981.

10. General Electric Company, Landsat-D Jitter Review, May 20-21, 1980.

11. T.C. Aepli, Approach to Geometric Performance Improvement, General Electric Company, PIR 1K51-LSD-684.